REFERENCES

[1] H. C. Casey, M. B. Panish, and J. L. Merz, "Beam divergence of the emission from double-heterostructure injection lasers," *J. Appl. Phys.*, vol. 44, pp. 5470–5475, 1973.
[2] P. A. Kirkby and G. H. B. Thompson, "The effect of double heterostructure waveguide parameters on the far field emission patterns of lasers," *Opto-Electron.*, vol. 4, pp. 323–334, 1972.
[3] G. A. Hockham, "Radiation from a solid-state laser," *Electron. Lett.*, vol. 9, pp. 389–391, 1973.
[4] L. Lewin, "Obliquity-factor for radiation from a solid-state laser," *Electron. Lett.*, vol. 10, pp. 134–135, 1974.
[5] ——, "Obliquity-factor correction to solid-state laser radiation patterns," *J. Appl. Phys.*, May 1975.
[6] J. K. Butler and J. Zoroofchi, "Radiation fields of GaAs–AlGa)As injection lasers," *J. Quantum Electron.*, vol. QE-10, pp. 809–815, Oct. 1974.
[7] T. Ikegami, "Reflectivity of mode at facet and oscillation mode in double-heterostructure injection lasers," *IEEE J. Quantum Electron.*, vol. QE-6, pp. 470–476, June 1972.
[8] D. Marcuse, *Light Transmission Optics.* New York: Van Nostrand-Reinhold, 1972, pp. 305–325.

Short Papers

Characteristic Impedance and Field Patterns of the Shielded Microstrip on a Ferrite Substrate

DAVID T. YEH AND DONALD M. BOLLE, SENIOR MEMBER, IEEE

Abstract—**The dispersion relation, field patterns, and current density at the interface of a shielded microstrip on ferrite substrate while operating at remanence is obtained and the characteristic impedance of such a structure is presented.**

In a paper by Minor and Bolle [1], the dispersion relation of a shielded microstrip on a ferrite substrate transversly magnetized in the plane of the substrate was analyzed. The method of solution used was to construct an appropriate modal expansion in each of the two media. The boundary conditions at the interface were then expressed in terms of two coupled integral equations which were subsequently solved by the method of moments. An estimate of 0.5-percent accuracy using a matrix as small as 5×5 was reported.

In this short paper, we obtain the characteristic impedance based on the theory of [1]. The earlier computer program was modified so as to yield numerical results for the characteristic impedance.

The model of the shielded microstrip is shown in Fig. 1. The waveguide walls and the strip are all presumed perfectly conducting. The strip is infinitely thin, and each of the two regions may be either dielectric- or ferrite-loaded. We define the characteristic impedance

Manuscript received September 25, 1974; revised February 7, 1975. This work was supported by the National Science Foundation under Grant GK-31591.
The authors are with the Division of Engineering, Brown University, Providence, R. I. 02912.

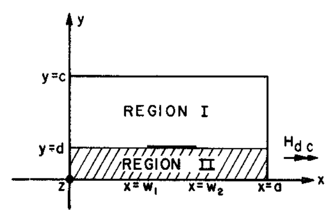

Fig. 1. The shielded microstrip.

of such a structure by (see Fig. 1)

$$Z_0 \triangleq \frac{V}{I} \tag{1}$$

where

$$V = -\int_0^d E_{IIy}\left(x = \frac{w_1 + w_2}{2}, y\right) dy \tag{2}$$

and

$$I = \int_{w_1}^{w_2} J_z^E(x)\, dx. \tag{3}$$

E_{IIy} is the y component of the electric field in region II. $J_z^E(x)$ is the axial electric current density. Both of these quantities may be calculated directly once the propagation factor β is obtained for a time dependence of the form $\exp[j\omega t]$. The path of integration taken for the voltage integral is at the midpoint of the strip with $x = (w_1 + w_2)/2$. The current I is the total axial current in the direction of propagation.

To ensure the correctness and establish the accuracy of the program and of the formulation, comparison with previous results was made. The physical dimensions of the structure are shown in the inset of Fig. 2. The characteristic impedance was computed for various dielectrics loading region II and with W/H (ratio of strip width to substrate height) as a parameter. The results obtained were compared to those obtained by Bryant and Weiss [2]. The figure shows that the disagreement is well within 3 percent for all cases except when $W/H \leq 0.5$. Although the error for narrow strips is much higher (5–7 percent), this may well be due in part to the inaccuracy incurred in transferring values from the graph of [2]. Also, it should be noted that Bryant and Weiss [2] considered unshielded microstrip line in contrast to the shielded microstrip line investigated here.

Having established such agreement for the isotropically loaded structure, computations were extended to the anisotropically loaded structure. The physical dimensions of the structure are shown in Fig. 3 along with the ω–β diagram. For the meaning of the search parameters consult [1]. Data are presented for the ferrite operating at remanence, i.e., $H_{dc} = 0.0$ Oe.

Since the applied dc magnetic field is zero, the ferrite introduces substantial anisotropy at low frequencies, i.e., at 1 GHz, $\chi = 0.0$, but $\kappa = -6.1614$, where χ and κ are the diagonal and off-diagonal components of the magnetic susceptibility tensor. The result of such anisotropy is readily observed from the dispersion diagram. A 10–20-percent difference in the values of the propagation constant is seen for opposing direction of propagation with $|\beta|$ larger for $\beta > 0$ than it is for $\beta < 0$.

As we were interested primarily in modes with zero cutoff, only the dispersion for low frequencies was investigated. The appearance of a slow wave $[|\beta/k_0| > (12.7)^{1/2}]$ in this guide is not unexpected since it also occurs in the stripless ferrite-loaded waveguide [3]. Also, in that the energy of this mode is predominantly concentrated in the region between the strip and the plate, it appears to be a perturbation of the TM_{00}, i.e., TEM, mode for the parallel-plane guide. The phase velocity of this mode is the free-space value modified by the dielectric constant. As is observed, this value is asymptotically approached as $\omega \to 0$. The results obtained agree in general with those obtained by Minor and Bolle [1] except in that their use of high dc magnetic fields, which facilitated comparison with previously published isotropic substrate data, resulted in near symmetry of the dispersion relation plot at low frequencies. The previously observed two modes of propagation [4] exhibiting no cutoff were again obtained from the dispersion relation for each direction of propagation.

The characteristic impedance of such a structure was then computed for the ferrite at remanence with $f = 1$ GHz. The result is displayed in Fig. 4. The increase of characteristic impedance with decreasing W/H ratio is to be expected since similar behavior is observed for the dielectrically loaded structure.

To obtain further insight into the behavior of the electromagnetic waves in such a structure, the field patterns and the current density at the interface were obtained.

The field patterns at $f = 1$ GHz for each of the modes exhibiting no cutoff are shown in Fig. 5(a), (b), (c), (d). The field patterns were obtained using a CALCOMP plotter. The absolute magnitude and the direction of the transverse electric and magnetic field intensities were obtained at the points of a grid structure in the transverse plane and are represented by the length and direction of the short lines. These field quantities were suitably scaled to fit the plotter format. It should be noted that only the field patterns near the stripline are shown. The boundaries shown in Fig. 5 do not therefore coincide with the perfectly conducting boundaries. The dots indicate the location of the microstrip edges inside the waveguide.

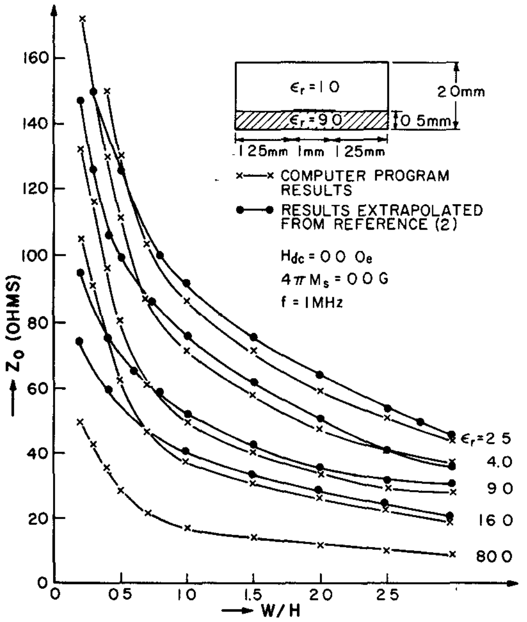

Fig. 2. Characteristic impedance of the shielded microstrip (W = strip width, H = substrate thickness).

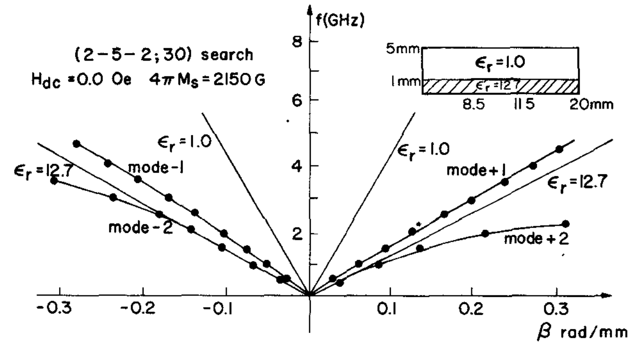

Fig. 3. Dispersion relation diagram for a shielded microstrip with ferrite substrate.

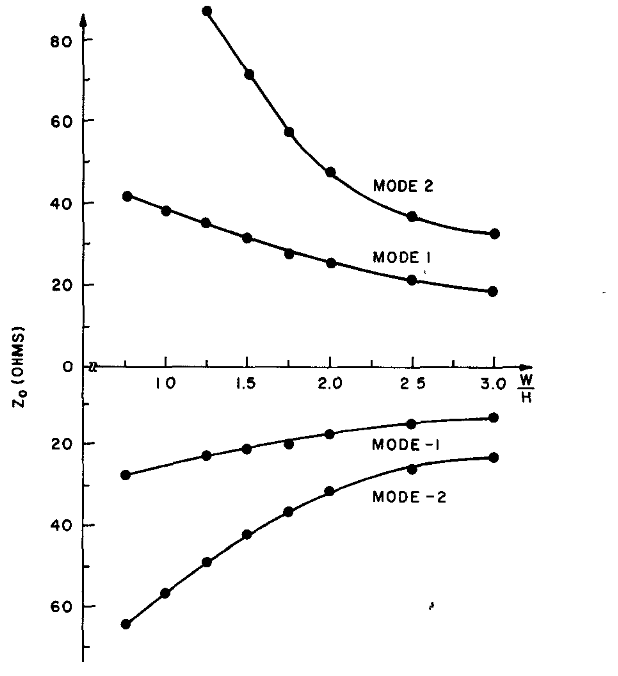

Fig. 4. Characteristic impedance of the ferrite-loaded shielded microstrip (H_{dc} = 0 Oe). (W = strip width, H = substrate thickness.)

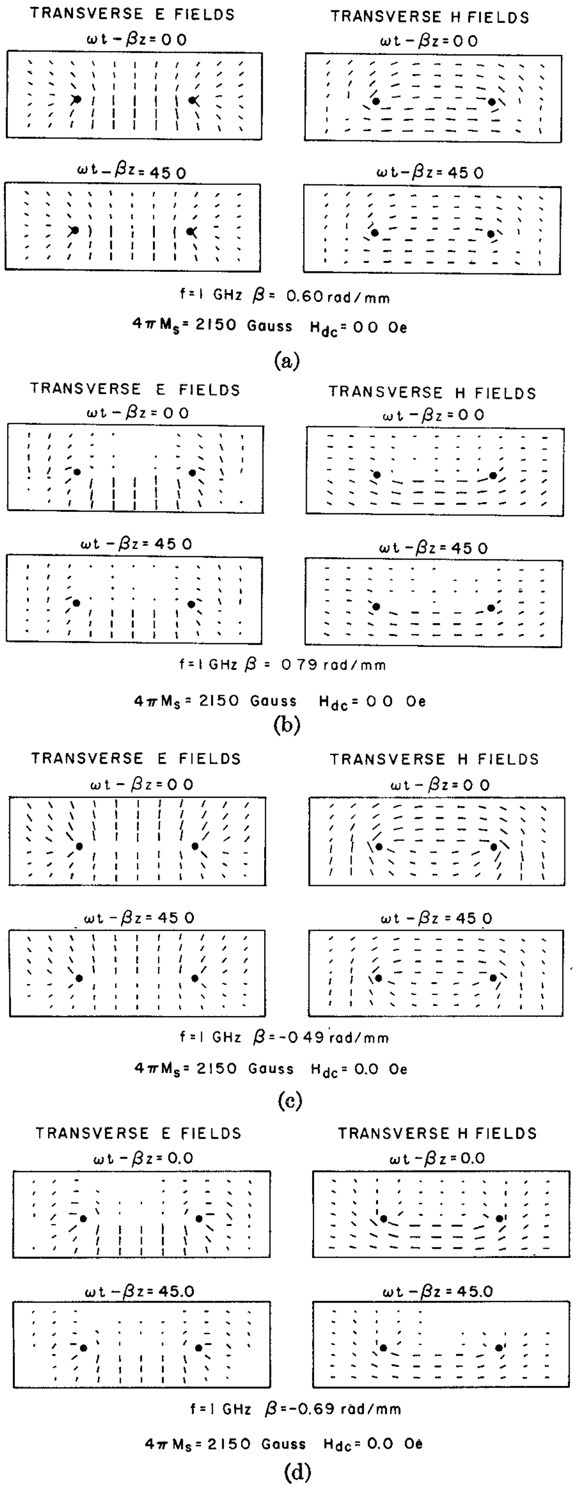

Fig. 5. (a) Transverse fields for mode 1. (b) Transverse fields for mode 2. (c) Transverse fields for mode −1. (d) Transverse fields for mode −2.

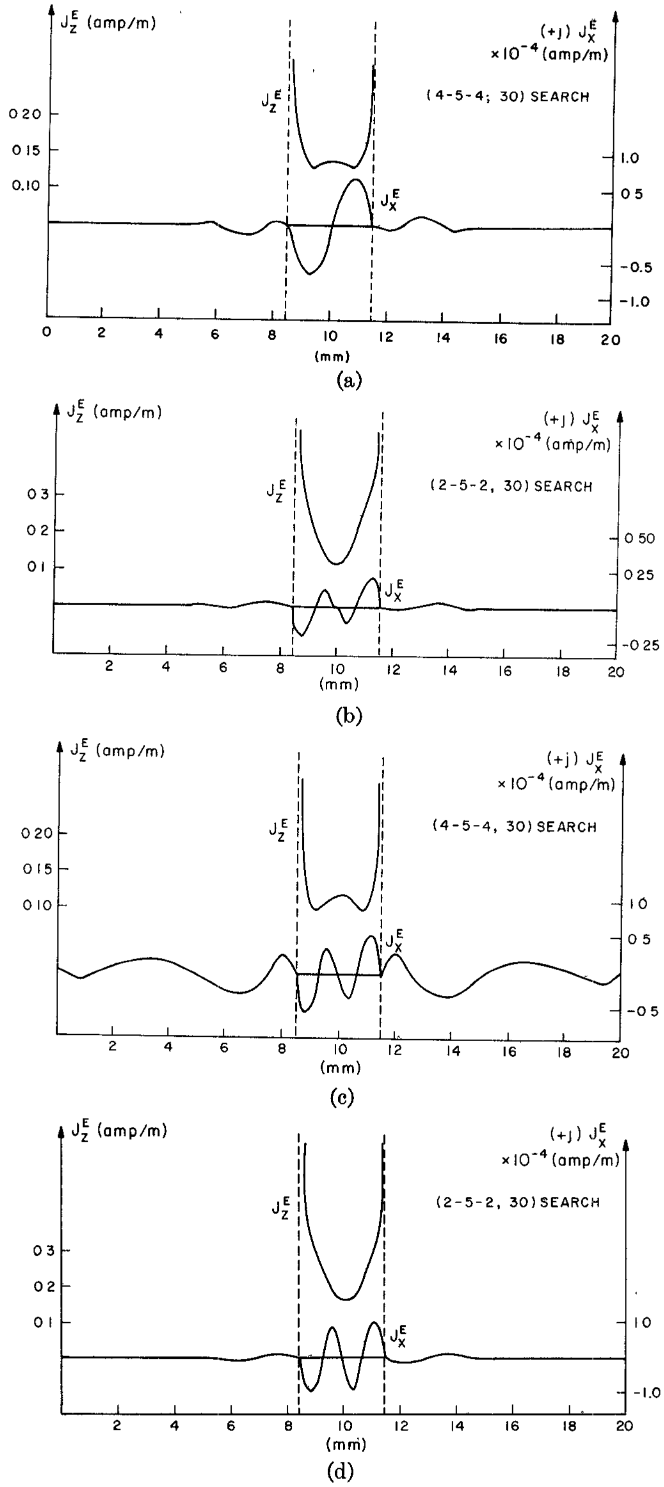

Fig 6. (a) The total electric current at $y = d$ for mode 1. (b) The total electric current at $y = d$ for mode 2. (c) The total electric current at $y = d$ for mode −1. (d) The total electric current at $y = d$ for mode −2.

The general characteristic of the field patterns are much as would be expected. The magnetic lines of forces encircle the strip, while electric lines of forces direct themselves towards (or away from) the strip. Both magnetic and electric fields are concentrated near the edges of the strip. In modes +2 and −2, both magnetic and electric fields are highly concentrated in the ferrite substrate directly under the strip. Since the field patterns are obtained for the low-frequency range (1 GHz), a quasi-TEM mode is expected and the magnitudes of the longitudinal field components were not significant.

In Fig. 6(a), (b), (c), (d), the instantaneous electric current at the interface for each mode are plotted for $f = 1$ GHz. As mentioned in [1], these graphs should not be expected to be as accurate as the eigenvalues (dispersion relation plot, Fig. 3). Since the total (top of strip plus bottom of strip) axial current is constructed from the eigenvector, it is by definition identically zero outside the strip. The total transverse current is constructed from the Fourier series over the entire waveguide width. One should especially note the difference in magnitude between the minimum of J_z^E and the maximum of J_x^E (note the different scale for J_z^E and J_x^E).

The program as written also allows inclusion of lossy media by only a slight modification since ϵ_r, κ, and χ are already written as complex variables. Limitation in time and money restricted the number of results that could be obtained.

REFERENCES

[1] J. C. Minor and D. M. Bolle, "Modes in the shielded microstrip on a ferrite substrate transversely magnetized in the plane of the substrate," *IEEE Trans. Microwave Theory Tech.* (*Special Issue on Microwave Integrated Circuits*), vol. MTT-19, pp. 570–577, July 1971.

[2] T. G. Bryant and J. A. Weiss, "Parameters of microstrip transmission lines and of coupled pairs of microstrip lines," *IEEE Trans. Microwave Theory Tech.* (*1968 Symposium Issue*), vol. MTT-16, pp. 1021–1027, Dec. 1968.

[3] G. Barzilai and G. Gerosa, "Modes in rectangular waveguides partially filled with ferrite," *IEEE Trans. Antennas Propagat.* (*Special Supplement—Symposium on Electromagnetic Theory*), vol. AP-7, pp. S471–S474, Dec. 1959.

[4] D. M. Bolle, "Recent advances in the theory of planar waveguiding structures in ferrite substrates," in *Proc. Sem. Int. Dispositifs Hyperfreq. a Ferrite, Dig.* (Toulouse, France, Mar. 1972), pp. D IV 1–7.

Capacitance of a Circular Disk for Applications in Microwave Integrated Circuits

SURESH R. BORKAR, MEMBER, IEEE, AND RICHARD F. H. YANG, FELLOW, IEEE

***Abstract*—The quasi-static solution for a circular disk separated from a ground plane by a dielectric substrate is studied using the dual integral equation approach. A simple expression for equivalent capacitance is determined.**

INTRODUCTION

The analytical study of disk resonators is of considerable importance for applications in integrated circuits. In order to determine the resonant frequency of such structures, it becomes necessary to obtain the value of capacitance [1], [2]. Recently, the determination of capacitance for a circular disk resonator was accomplished using computer calculations based on a numerical approach in spectral domain [1], [3]. Although capacitance was determined readily, it appears that the determination of actual surface charge densities and potential functions may warrant inversion of matrices of large orders.

The main complication in such a class of problems arises because of the mixed boundary conditions involved. Various approaches have been put forth in the past to circumvent this complexity. Rikitake [4] used the relaxation method for studying electromagnetic induction in a plane sheet with a circular aperture. For a two-dimensional problem in Cartesian coordinates, use was made of conformal mapping [5]. A method using multiple partial images has been reported [6]. The capacitance of disk resonator in free space has also been obtained [7]. In this short paper, a convenient method for an accurate solution to the disk resonator is developed using dual integral equations [8]. A major advantage lies in the fact that capacitance, charge densities, and field functions are determined in terms of a quickly convergent series.

Manuscript received March 13, 1974; revised March 20, 1975.

S. R. Borkar was with the Department of Electrical Engineering, Illinois Institute of Technology, Chicago, Ill. He is now with the Zenith Radio Corp., Chicago, Ill. 60639.

R. F. H. Yang was with the Department of Electrical Engineering, Illinois Institute of Technology, Chicago, Ill. He is now a Consultant in electromagnetics at 10021 West 146th St., Orland Park, Ill. 60462.

FORMULATION

Consider the geometry shown in Fig. 1 for a circular disk resonator of radius "a," separated from a ground plane by a dielectric material. Without loss of generality, the radius is assumed to be unity. The disk is charged to potential V_0. The potential functions are considered to be $\phi_1(r,z)$ and $\phi_2(r,z)$ for $z > d$ and $0 < z < d$, respectively. Because of circular symmetry, the Hankel transforms of these functions may be defined as

$$\bar{\Phi}_{1,2}(\alpha,z) = \int_0^\infty \phi_{1,2}(r,z) J_0(\alpha r) r \, dr. \tag{1}$$

Using the boundary conditions $\bar{\Phi}_2(\alpha,0) = 0$ and $\bar{\Phi}_1(\alpha, +\infty) = 0$, the following expressions for potentials are obtained:

$$\bar{\Phi}_2(\alpha,z) = A(\alpha) \sinh \alpha z, \qquad 0 < z < d \tag{2}$$

$$\bar{\Phi}_1(\alpha,z) = B(\alpha) \exp[-\alpha(z-d)], \qquad z > d. \tag{3}$$

The unknowns $A(\alpha)$ and $B(\alpha)$ are to be determined from the following boundary conditions. At the interface $z = d$,

$$\phi_1(r,d) = \phi_2(r,d). \tag{4}$$

In particular,

$$\phi_1(r,d) = \phi_2(r,d) = V_0, \qquad 0 < r < 1. \tag{5}$$

Also at $z = d$

$$\frac{\partial \phi_1(r,d)}{\partial z} - \epsilon_r \frac{\partial \phi_2(r,d)}{\partial z} = 0, \qquad r > 1. \tag{6}$$

Clearly from (4)

$$A(\alpha) \sinh \alpha d = B(\alpha) \tag{7}$$

and using (6) and (7), one can obtain the following dual integral equations

$$\int_0^\infty \frac{\alpha^{-1} \sinh \alpha d}{[\sinh \alpha d + \epsilon_r \cosh \alpha d]} \cdot f(\alpha) \cdot J_0(\alpha r) d\alpha = V_0, \qquad 0 < r < 1 \tag{8}$$

and

$$\int_0^\infty f(\alpha) \cdot J_0(\alpha r) d\alpha = 0, \qquad r > 1 \tag{9}$$

where

$$f(\alpha) = \alpha^2 A(\alpha)[\sinh \alpha d + \epsilon_r \cosh \alpha d]. \tag{10}$$

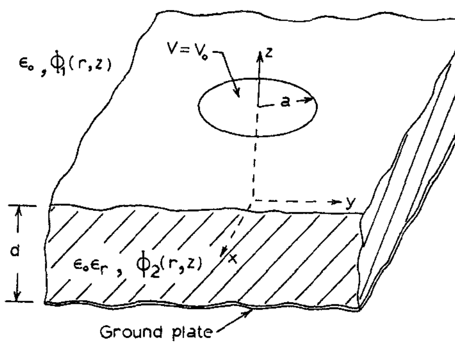

Fig. 1. Geometry of the problem.